View metadata, citation and similar papers at core.ac.uk
brought to you by CORE
provided by LJMU Research Online

pss-Header will be provided by the publisher

Review copy – not for distribution

(pss-logo will be inserted here by the publisher)

Carbon nanoparticles fabricated by infrared laser ablation of graphite and polycrystalline diamond targets

Mariusz Dudek [*,1], Adam Rosowski [2,3], Anna Koperkiewicz [1], Jaroslaw Grobelny [4], Radoslaw Wach [5], Martin Sharp[2], Paul French [2], Lukasz Janasz [6] and Marcin Kozanecki [6]

[1] Lodz University of Technology, Institute of Materials Science and Engineering, 1/15 Stefanowskiego Street, 90- 924 Lodz, Poland
[2] Liverpool John Moores University, General Engineering Research Institute, Byrom Street, Liverpool L3 3AF, United Kingdom
[3] SPI Lasers, 3 Wellington Park, Tollbar Way, Hedge End, Southampton, Hampshire SO30 2QU, United Kingdom
[4] University of Lodz, Department of Materials Technology and Chemistry, 163Pomorska Street, 90 236 Lodz, Poland
[5] Lodz University of Technology, Institute of Applied Radiation Chemistry, 15 Wroblewskiego Street, 93-590 Lodz, Poland
[6] Lodz University of Technology, Department of Molecular Physics, 116 Zeromskiego Street, 90 924 Lodz, Poland

Received ZZZ, revised ZZZ, accepted ZZZ
Published online ZZZ (Dates will be provided by the publisher.)

Keywords carbon nanoparticles (CNPs), Liquid Phase – Pulsed Laser Ablation (LP-PLA), graphite, Raman spectroscopy, fluorescence spectroscopy

* Corresponding author: mariusz.dudek@p.lodz.pl, Phone: +48 42 631 3071, Fax: +48 42 631 3038

This paper presents the results of carbon nanoparticles (CNPs) production by infrared laser ablation of a graphite or a polycrystalline diamond target, submersed in one of two solvents, water or isopropanol. The targets were irradiated using a SPI fibre laser with a wavelength of 1064 nm being operated at different average powers. After laser-assisted synthesis of CNPs, the resulting colloids, i.e, particles in a liquid medium, were examined using the analytical techniques of dynamic light scattering, UV-Vis, Raman spectroscopy and fluorescence spectroscopy.

The results show that the properties of CNPs strongly depend on processing conditions of the Liquid Phase – Pulsed Laser Ablation (LP-PLA) process. In particular, the size of nanoparticles produced are affected by the processing parameters of the laser ablation. The results show that the laser processing of a graphite target in deionised water and in isopropanol produces carbon nanoparticles with properties that are beneficial for various biochemical and biomedical applications.

Copyright line will be provided by the publisher

1 Introduction Carbon-based materials in the form of thin coatings, nanotubes, graphene layers and nanoparticles have increasingly played an important role in both a countries modern economy performance and in science in general [1-5]. Specifically, carbon nanoparticles (CNPs) have emerged as a new class of carbon-based nanomaterials due to their properties such as large surface/volume ratio, low toxicity and biocompatibility. The superior biological properties of CNPs have significantly contributed to a replacement of traditional semiconductor quantum dots in bio-imaging, biosensor and biomolecule/drug delivery applications [4, 6-9].

Many biological applications require the high surface activity of the CNPs. One of the well-known methods used to synthesise them is the Liquid Phase – Pulsed Laser Ablation (LP-PLA) process. This is a simple processing method, and thanks to the number of different processing parameters that can be varied, with respect to types of lasers (wavelength, pulse duration, frequency) and scanner parameters, efficient, fast production of CNPs can be achieved. It has been observed that the control of particle size (homogeneity) and their surface morphology, material allotropes, optical properties and functionalisation are strongly influenced by the organic solvents used as the liquid media [1, 10-15]. LP-PLA process is an example of a

Copyright line will be provided by the publisher

top-down method for CNPs synthesis similar to processes applying arc discharge or electrochemical oxidation processing [4, 16-17].

The LP-PLA process can by described [11, 18] as the ablation (removal) of material in the form of a plasma plume as a result of the incidence of a laser beam onto a materials surface. When water is used as a liquid medium, the high temperature of the plume results in the ionization and vaporization of the water at the plume–liquid interface. This produces water vapour and atomic molecular hydrogen or oxygen within the water-plasma region. This water 'plasma' mixes with the plume plasma above the laser beam-material interaction site and as a result a chemical reactions takes place between the water 'plasma' and the ablated species plasma. The characteristic of LP-PLA process can by compared to the ablation within a vacuum or the ablation process within a controlled atmosphere, in this case the processing media is a liquid, an organic solvent, and in one step NPs are producing and functionalised.

The present work focuses on the use of a laser assisted process for producing NPs, LP-PLA, a very simple and cheap method for the preparation of carbon nanoparticles. The effect of laser power, type of target and solvent (in which target was submersed during synthesis process) was studied. Dynamic light scattering (DLS) and UV-Vis, Raman as well as fluorescence spectroscopy were used to characterize the nanoparticles.

Both deionised water and isopropanol was used in the LP-PLA experiments because OH groups easily form in these oxygen-containing liquids. OH groups will stimulate etching of CNPs surface, and create atomic hydrogen which playing a role analogous to that in conventional diamond CVD process [19, 20]. Moreover, water is a non-toxic liquid which is important for obtaining colloids for biomedical applications. Isopropanol exhibits good miscibility in water as well as in organic solvent, which allows for easy transfer of the manufactured nanoparticles to both inorganic and organic phases.

2 Materials and methods The CNPs were prepared using infrared laser ablation of graphite or polycrystalline diamond targets submersed in one of two solvents: deionised water or isopropanol.

The experimental set-up consisted of a 20 W G3 SPI pulsed laser system with a wavelength of 1064 nm, line band width < 4 nm. The laser systems pulse duration is in the range of 10 ns – 200 ns, and has an operating frequency in the region of 1 kHz – 500 kHz, depending on pulse duration used in processing. A beam expander delivering an 11 mm diameter beam to a GSI Lightning scanner head and a Linos F-Theta 100 mm focusing lens. The beam quality, M^2 of the laser in single mode was < 1.6. The experimental set up is shown in Figure 1.

The diameter of the laser spot on the substrate surface was about 30 µm. The scanner head with an F Theta lens allowed for moving the focused beam over the substrate keeping the focal position on the substrate surface. A scanning area of 6 mm x 6 mm, was processed with a distance of 30 µm between each scanned lines this ensured that the whole of the processing area was covered. Scanning the laser beam over the surface was repeated 1250 times giving a total exposure time of ~2000 seconds. This process ablated material for the surface and created the nanoparticles - the parameters for both laser and scanner used to synthesis of CNPs are summarising in Table 1. After LP-PLA synthesis, the obtained colloids of CNPs in their respective liquid medium, were examined by various techniques.

Table 1 The parameters of laser and scanner used to synthesis of CNPs

Parameters	Value
pulse duration	200 ns
frequency	25 kHz
average power	adjustable in range 0.18 - 7.52 W
spot size	35 µm
scan speed	600 mm/s
scan grid	30 × 30 µm

The size of particles and their size distribution were measured using a dynamic laser scattering Nano ZS zetasizer (Malvern Instruments). The following parameters were used: laser wavelength - 633 nm (He-Ne laser line), scattering angle - 173º. Nano ZS zetasizer system was also used to measure zeta potential. The cumulate analysis of data (particle size, contents of fraction, polydispersity index and Z-potential) was performed using the International Standard on Dynamic Light Scattering ISO13321 and ISO22412 [21, 22] as guidance. Optical absorption spectra of colloids were recorded in a quartz cuvette (10 mm path length, Helma) with Varian Cary 5000 UV-Vis-NIR spectrophotometer with a 600 nm/min scan rate and a scan step of 1 nm. The scan range was 200–1400 nm.

Spectrofluorometric studies were performed using a FLS 980 fluorescence spectrometer (Edinburgh Instruments Ltd.). The excitation spectra were collected using a scan step of 1 nm and a 2 nm excitation slit width. An emission slit width of 5 nm was also used during the taking of these readings. Emission spectra were obtained with the same scan step and with slits width of excitation and emis sion arms of 5 and 2 nm, respectively. Acquisition time was 2 s/point.

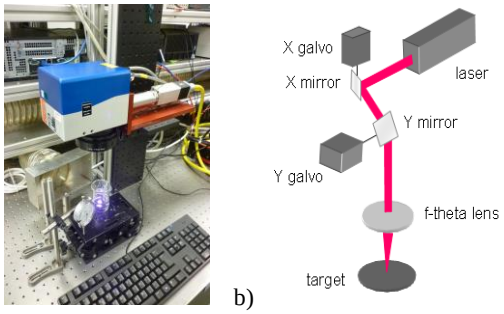

Figure 1 The Stations-up used to produce nanoparticles: a) picture of the system b) schematic of the system

Copyright line will be provided by the publisher

Table 2 Effect of laser power on the characteristics of CNPs produced from graphite and polycrystalline diamond target submersed in deionised water (* in isopropanol)

No.	Laser power (W)	Particle size – AFM images (nm)	DLS			
			Particle size (nm)	Contents (%)	Polydispersity index	Z-potential (mV)
graphite target						
1	0.18	~89 ~532	100 ± 13 470 ± 70	75 25	0.596	-19.97 ± 0.26
2	1.37	~67	75 ± 20	100	0.246	-18.40 ± 0.46
3	3.09	~71 ~196	66 ± 13 170 ± 50	75 25	0.251	-23.43 ± 0.55
4*	3.09	~107	82 ± 12	100	0.493	-30.23 ± 1.14
5	4.59	~74	75 ± 20	100	0.261	-22.13 ± 2.06
6	7.52	~100	~ 100	100	0.513	-16.30 ± 0.26
polycrystalline diamond target						
7	3.09	~70 ~175	60 ± 11 163 ± 37	67 33	0.239	-19.07 ± 0.42
8	5.27	~81 ~208	66 ± 14 142 ± 37	62 38	0.202	-17.60 ± 0.89
9	7.52	~74 ~170	74 ± 19 163 ± 39	75 25	0.237	-22.07 ± 1.07

The shape, size and distribution of CNPs were also investigated using scanning electron microscopy (SEM, Nova NanoSEM 450, FEI, accelerating voltage of 30 kV) equipped with a detector for scanning transmission electron microscopy (STEM II). The STEM detector located under the sample allows detection of electrons passing through the sample as in the case of transmission electron microscopy (TEM). Samples for STEM investigations were prepared as follows: 4 μl of the colloid were deposited onto carbon-coated copper grids (300 mesh). The suspension was left for 1 h for solvent evaporation. Then, the samples were cleaned under a vacuum for 60 min to remove any excess solvent.

After LP-PLA processing the graphite and polycrystalline diamond targets, the colloid was poured onto a glass slide and was left to dry. The CNPs were then investigated using a Solver PRO, NT-MDT atomic force microscope with 320 kHz resonance frequency μ-mash silicone cantilevers. AFM measurements were performed in tapping mode with the parameters being varied depending on the measured sample. Sizes of the particles were estimated using the Gwyddion 2.38 software and applied Out's thresholding method.

Glass samples with dry CNPs were also investigated using a Renishaw inVia Raman Microscope equipped with 532 nm laser set up in a backscattering geometry. The applied wavenumbers ranged from 100 cm^{-1} to 3200 cm^{-1}. All measurements were carried out at room temperature and in an air atmosphere.

3 Results and discussion

3.1 DLS and Raman spectroscopy The colloids produced by the LP-PLA process were examined using the a number of different techniques. Attention was focused on the effect of laser power on general characteristics of the nanoparticles, produced from the graphite target submersed in deionised water with the other remaining process parameters held constant (see Table 1). The main results are summarized in Table 2, and good agreement in the size of CNPs obtained by two techniques was observed. Figure 2 shows two examples of size distribution of CNPs produced with laser power of 0.18 and 4.59 W analysed by DLS technique, and shows that the graphite processed at 0.18W, two distinct populations of CNPs are observed. AFM and STEM analysis confirms this observation. Estimated size of CNPs processed with 0.18 W based on STEM images presented in Figure 2 shows is equal 82 ± 19 nm – for the smaller fraction, and 499 ± 116 nm – for the bigger fraction (respectively top and bottom image). It is also observed that the shapes of the CNPs are irregular.

It can be seen in Table 2 that for graphite processed at 0.18 and 3.09 W, some of the samples, using the DLS analytical technique, shows the presence of two populations of sizes for CNPs. Estimated contribution of them indicates that the smaller fraction of CNPs is always dominant and independent of the laser power used in the LP-PLA process. Relatively broad size distribution of obtained CNPs is reflected in the high values of polydispersity index, which is found to be equal 0.25 – 0.60 - see Table 2. For the water colloids, the maximum value of polydispersity index was estimated at twice the limit value of the power used in the LP-PLA processing (at 0.18 and 7.52 W), and the minimum for intermediate values. This indicates that at lower power small modified and large unmodified CNPs were produced (two fractions with a large difference in size – see Figure 2), whereas at higher laser power of LP-PLA process modified CNPs with a size of about 100 nm.

Copyright line will be provided by the publisher

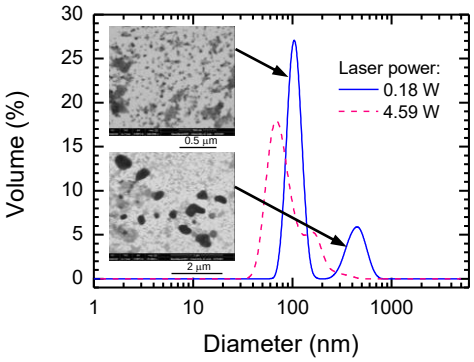

Figure 2 Size distribution of CNPs obtained with use of graphite target submersed in deionised water at two laser power – the particle distribution profile complements data summarized in Table 2. Inside: STEM images shows two fraction of CNPs produced at 0.18 W laser power

Considering only the smaller of the two size populations for the CNPs produced, in water using a graphite target, one can conclude that generally their size depends on the mean power used for laser machining the graphite target. It is clear, that the relationship between laser power and a CNPs size is not monotonous, with the minimum value at about 3 W, the same relationship also exists for the polydispersity index.

Taking into account both identified fractions of CNPs produced in water from graphite target one can see that the LP-PLA process at low laser power leads to the removing of CNPs from the target surface without modification of their size, a larger fraction CNPs is seen at 0.18 W. With increase in laser power, a modification process, for carbon nanoparticles processed in a liquid media is observed [10]. In our case with an increase in laser power, up to 3 W, particle size reduction is observed. With further laser power increase the size of nanoparticles increases and the modification of the particles during LP-PLA process leading to a growth in nanoparticles size. Measured values of zeta potential (Table 2) for all colloids remained at the same level (~20 mV absolute value). The ablation process performed in isopropanol leads to a higher absolute value of zeta potential in comparison with processing in deionised water. For the process performed at 3.09 W of laser power (Table 2) we obtain respectively value -30.23 mV and 22.13 mV. Considering the values of zeta potential it should be noted that nanoparticles are characterized by their emerging instability or by a tendency of the particles to aggregate, which is reflected in the presence of the high fraction size.

LP-PLA processing of the graphite target in isopropanol with 3.09 W of laser power has an important impact on nanoparticle size. In this case, a population of particles with the average sizes of 82 nm was obtained, whereas laser processing using the same power for the graphite target in deionised water lead to production of two populations of CNPs with the average sizes of 66 and 170 nm (Table 2).

The LP-PLA process, carried out at a high laser power, leads to modification of the carbon nanoparticles during this processing. Raman spectroscopy was used to bring detailed information about the phase structures of the prepared CNPs. Figure 3 shows a comparison of Raman spectra of CNPs obtained by two laser powers with spectra of the graphite target before and after ablation when the target was submersed in deionised water. Generally, LP-PLA processed nanoparticles can be described as a graphite nanoparticles with a high content of disordered graphite with a spectra having an increased peak around 1350 cm^{-1} (D band) with simultaneous disappearing peak about 2700 cm^{-1} (2D band). In the case of spectra presented in Figure 3, bands characteristic of fullerenes are also observed. The number and position of lines on the spectra indicate that

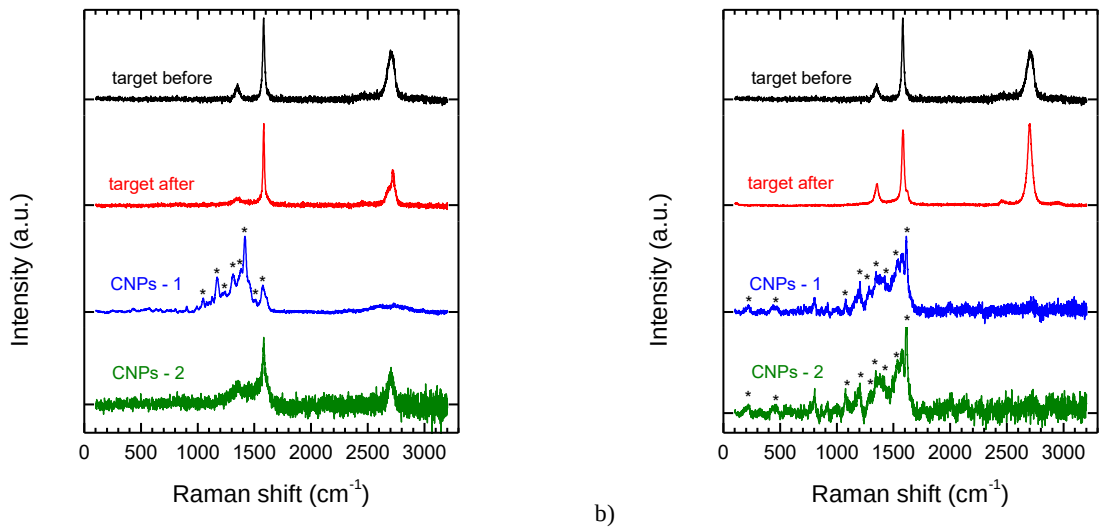

Figure 3 Fullerene like Raman spectra of CNPs in comparison with graphite target before and after LP-PLA process. The spectra illustrate data summarized in Table 2, for graphite target submersed in deionised water and laser power a) 0.18 W and b) 4.59 W (asterisk indicates fullerene peaks)

Copyright line will be provided by the publisher

CNPs contain fullerenes with reduced molecular symmetry and showing more Raman bands being active [23]. Depending on parameters of LP PLA process, the strongest lines are observed at 1416 cm^{-1} and 1612 cm^{-1} for laser powers 0.18 W and 4.59 W respectively. Typical the line attributed to fullerene C60, a sharp line around 1463 cm^{-1} is not clearly visible in the spectra. This is probably due to it being it being overlapped by the other lines.

The LP-PLA process at the power 3.09 W was conducted for a graphite target submersed in deionised water and isopropanol. In both cases a band typical for graphite in Raman spectra (not shown here) was identified. The effect of using isopropanol is manifested in the significant intensity decrease of the 2D peak (~ 2700 cm^{-1}) in Raman spectrum of CNPs. Previously it was observed in the case of processing with the target submersed in deionised water. Part of the spectra with D band (~1350 cm^{-1}) and G band (~1580 cm^{-1}) was identical.

Finally, it should be stated that the LP-PLA process also modifies the graphite target. Figure 3 shows that laser treatment leads to modification of the graphite surface – the effect of the modification of the processed target is strongly visible in the case of CNPs prepared from polycrystalline diamond. As Figure 4 shows, D band, G band and 2D band are clearly seen in Raman spectra of target after the ablation process.

Laser ablation, leading to the formation of CNPs was also carried out for polycrystalline diamond target submersed in deionised water. The characteristics of the products produced from this processing is summarised in Table 2. Two populations of particles with the size in the range 60-74 nm and ca. 155 nm were identified in the resulting colloids. The size of the CNPs from the smaller population increases with laser power for LP-PLA process almost linearly, while the average size of the CNPs with respect to the larger size population was observed to be practically independent of power laser. Thus, a straightforward relation could not be found for size distribution, with respect to the content of both populations, as well as polydispersity index and the process conditions for the case of the diamond target. Very similar values of zeta potential was also obtained for CNPs prepared from the diamond target, being somewhat similar to the graphite in terms of instability in water.

The Raman spectra for CNPs produced from the diamond target at two different laser powers are shown in Figure 4. Only two peaks – D band and G band in Raman spectra exist. It should be stated that a diamond peak (1332 cm^{-1}) was not identified in any spectrum of these CNPs. However, there is a correlation between Raman spectra of CNPs and polycrystalline diamond target after LP-PLA processing (it observed graphitization process of polycrystal diamond target). The higher intensity of G band in target spectrum leads to CNPs with a higher G peak. The intensity ratio (I_D/I_G) which is commonly used to correlate structural purity, as proposed by Ferrari and Robertson [24] indicates that an amount of sp^3 bonds increases from 34% (at 3.09 W) to 40% (at 7.52 W) with an increase in laser power. Whereas the sizes of the nanoparticles obtained from the above-mentioned relationship was estimated as 3.1 nm at 3.09 W and 4.5 nm at 7.52 W of laser power. These values are far from the NPs sizes estimated by DLS. Two scenarios may be proposed to explain this disagreement. The first one assumes an aggregation of smaller CNPs with a size of few nm (found by Raman spectroscopy) into larger clusters with size of 60-100 nm (observed by DLS). The second scenario assumes that the CNPs prepared by laser ablation have complex shapes and could not be modelled by a simple sphere, but rather as a blackberry-like structure. Both are probable taking it into account that the optical phonons are the basis to determine CNPs size by Raman spectros copy. It means that the small parts of

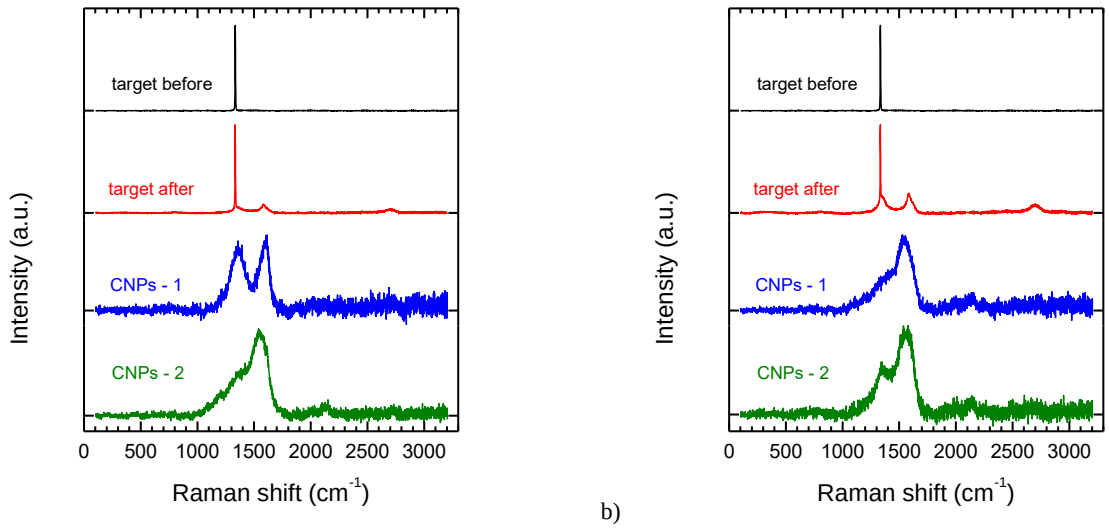

Figure 4 Raman spectra acquired for CNPs obtained from polycrystalline diamond target. The LP-PLA process with power a) 3.09 W and b) 7.52 W

Copyright line will be provided by the publisher

fractal or porous particles or aggregates give a Raman spectrum similar to the spectrum of separate CNPs of a size equal to these smaller particles. The DLS method is based on the measure of particle mobility and it is insensitive to the structure complexity, particles are assumed to be spherical or cylindrical. Moreover, the sizes of CNPs measured by DLS are usually overestimated, as the hydrodynamic radius of a moving objects is measured. It means that the size determined by DLS represents a size of nanoparticle expanded by the solvation sphere moving together with the particle.

3.2 Fluorescence spectroscopy The CNP colloids with obtained using LP-PLA process were also characterized by UV-Vis and fluorescence spectroscopy. UV-Vis measurements confirmed that the maximum absorbance existed below the threshold of operation of the spectrometer and the obtained spectra (not shown here) are similar to those published previously [8, 14, 25]. In the case of fluorescence measurements, figure 5 shows excitation and emission spectra for CNPs prepared using two laser powers 0.18 and 3.09 W which correspond to the largest and the smallest produced CNPs respectively. The highest fluorescence intensity was recorded at the excitation wavelength 275 nm, which shows the emission maximum at 315 nm for the colloid prepared at 0.18 W of laser power. In the case of colloid prepared at 3.09 W, the maximal emission was observed at 465 nm for excitation wavelength 310 nm. The coupling of two fluorescence lines visible on some emission spectra (see inserts in Figure 5) proved the presence of the two populations of CNPs in the samples. This is consistent with DLS measurements.

Figure 6 presents normalised emission spectra of CNPs prepared with various laser powers. Normalisation was done using the low energy maxima located between 400-550 nm. Practically for all of the samples two emission lines are visible. The insert in Figure 6 shows a relationship between positions of the emission bands versus CNPs size determined by DLS. Based on this graph, emission at about 300 nm for nanoparticles prepared at 1.37 W and 4.59 W can be assigned to sizes in the range from 650 to 700 nm. This mean that the long tail towards particle sizes with a higher value, visible on the graph of the distribution of the nanoparticles, has a significant influence on fluorescence emission.

The origin of the optoelectronic behaviour of carbon nanoparticles is still under discussion, thus a common interpretation of their fluorescence spectra is not simple [26]. The most popular hypothesis proposed to explain the origin of the photoluminescence of carbon nanoparticles has taken under consideration, such reasons as: size of nanoparticles (quantum effect), structural defects, surface states (including defects, functional groups passivation effects etc.), different degrees of π-conjugation, or electron–hole recombination localized within small sp^2 carbon clusters embedded within a sp^3 matrix [4, 27-32]. It was found that the emissive traps (centres of emission) were depend ent on the synthetic methods and the post-treatment. It is also important to mention that the emission properties of

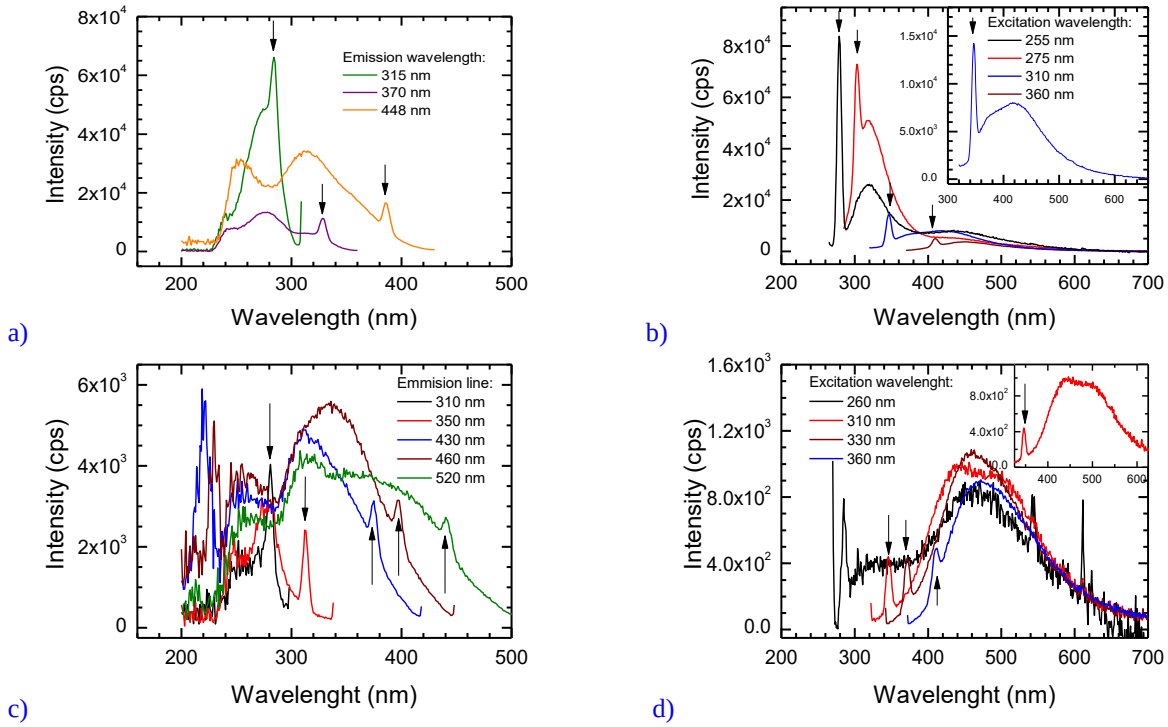

a) b) c) d)

Figure 5 Excitation (left) and emission (right) spectra of CNPs prepared with various laser powers: 0.18 W (respective a and b) and 3.09 W (c and d). Arrows indicate Raman line of water. Inserts present the emission spectra proving the presence of two fractions of CNPs

Copyright line will be provided by the publisher

carbon nanoparticles may be strongly depended on their electrical proprieties. For semiconducting carbon quantum nanodots, the spectral emission, is size-dependent and usually red-shifted with increasing size [27]. Calculations done for graphene fragments proved that such behaviour is related to the reduction of energy gap between HOMO and LUMO states as a result of an increase in particle size [27]. Calculations agreed well with experimental spectra for carbon quantum dots smaller than 3 nm. Recently Wang and Hu [26] showed that the emission spectra of carbon nanoparticles prepared from a polymeric precursors exhibit blue-shift with increasing size. To explain this untypical behaviour a calculation of the two series as model particles were performed: with a graphitized core and with an amorphous core. It was found that the fluorescence in the graphitized-core particles is red shifted with increasing nanoparticle size, while in a case amorphous-core the opposite effect occurs. Thus one can conclude from these calculations that the LP-PLA method used in these experiments produce a significant number of carbon amorphous nanoparticles.

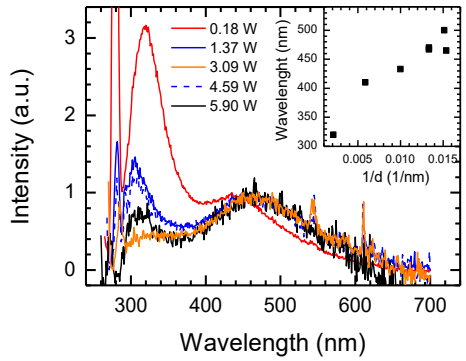

Figure 6 Normalized emission spectra of CNPs prepared with various power laser acquired with excitation wavelength 257 nm. Dependence of the wavelengths corresponding to the fluorescence maxima vs. size of CNPs determined by DLS is presented as insert

According to Deng et al. [33] double luminescence peak located between 400-550 nm may be interpreted as a coupling of both fluorescence (higher energy component with a maximum at 440-450 nm) and phosphorescence (lower energy component with a maximum at 500-520 nm). The phosphorescence are efficiently excited with the UV light (240-380 nm) – compare to the excitation spectrum recorded for emission at 520 nm. Such optical behaviours may be attributed to the n→π* transition of carbonyl groups typically located at the surface of carbon nanoparticles.

Fluorescence measurements allows for a discussion of the influence of the solvent used during LP-PLA process on the characteristics of CNPs. Figure 7 presents normalised to maxima excitation and emission spectra of the CNPs dispersed in the two various solvents: water and isopropanol. For CNPs dispersed in isopropanol only one emission line is visible independently on the excitation wavelength. This contrasts with two lines in the emission spectrum recorded with excitation wavelength 310 nm (Figure 7b) visible in the case of CNPs in water. Also excitation spectrum collected for emission line 520 nm confirms the presence of at least two populations of CNPs. These results are consistent with DLS (see Table 2) and Raman spectroscopy data. The obtained Raman spectra for CNPs in both solvents are almost identical in the case of D and G band. The spectra only differs for the existence of the 2D band in the spectra of nanoparticles manufactured from the graphite target submersed in deionised water, for isopropanol this band is not observed.

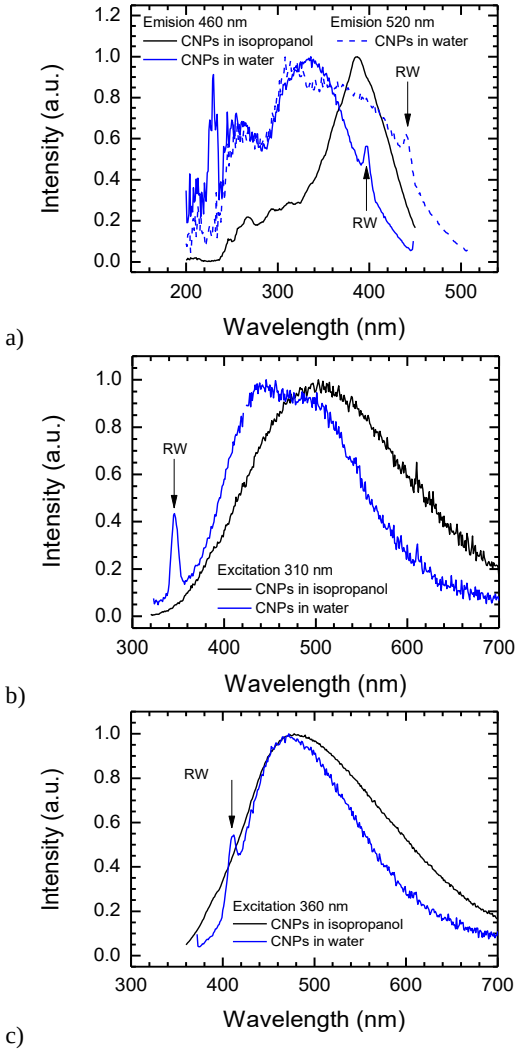

Figure 7 Influence Excitation spectra of CNPs dispersed in water and isopropanol acquired for the emission line 460 nm, for CNPs dispersed in water excitation spectrum for the emission line 520 nm was additionally attached to shown discrete character of the spectrum. b) and c) Emission spectra of CNPs dispersed in water and isopropanol excited with wavelengths 310 and 360 nm respectively. All spectra were normalized to maxima. Lines marked as RW corresponds to Raman signal of water

Copyright line will be provided by the publisher

4 Conclusions The presented results show that in the laser ablation process of graphite and polycrystalline diamond targets we can obtain stable colloids of carbon particles, with different characteristics in terms of size and phase structures. Thus we can synthesize CNPs with size lower than 100 nm, including a wide spectrum of allotropic forms of carbon. However the best results (one fraction with size about 75 nm) with fullerene like nanoparticles was obtained for LP-PLA process with a graphite target submersed in water with a laser power about 4.6 W.

For the graphite target submersed in water we can identify three stages of CNPs formation. In the first instance we observe (in particular at low laser power), removal of material from the target surface not associated with particle modification. Next, the laser impulse during the LP-PLA process interacts with the target leading to its modification. In last stage, we observe the formation of nanoparticles and their migration to the surrounding solutions. It should be emphasized that the last two steps occur simultaneously.

Fluorescence spectroscopy measurements indicate that LP-PLA process allows for synthesis of CNPs colloids with emission spectra in wide range of wavelength. This result confirms that these nanoparticles are interesting materials as markers in biomedical application. An untypical blue shift of the fluorescence maxima with increasing nanoparticle size may be credited to a high content of amorphous structures (or numerous structural defect) in LP-PLA processed carbon nanomaterials. A strong phosphorescence contribution suggests that the surface of a prepared carbon nanoparticles forms a carbonyl group conjugated with an aromatic structure.

References

[1] P.R. Willmott, J.R. Huber, Reviews of Modern Physics **72**, 315 (2000).

[2] Y.P. Sun, B. Zhou, Y. Lin, W. Wang, K.A.S. Fernando, P. Pathak, M.J. Meziani, B.A. Harruff, X. Wang, H. Wang, P.G. Luo, H. Yang, M.E. Kose, B. Chen, L.M. Veca, S.Y. Xie, Journal of the American Chemical Society **128**, 7756 (2006).

[3] Y.P. Sun, X. Wang, F. Lu, L. Cao, M.J. Meziani, P.G. Luo, L. Gu, L.M. Veca, Journal of Physical Chemistry **C 112**, 18295 (2008).

[4] S.N. Baker, G.A. Baker, Angewandte Chemie International Edition **49**, 6726 (2010).

[5] D. Pech, M. Brunet, H. Durou, P. Huang, V. Mochalin, Y. Gogotsi, P. Taberna,P. Simon, Nature Nanotechnology **5**, 651 (2010).

[6] Y. Xu, L. Yang, P.G. He, Y.Z. Fang, Journal of Biomedical Nanotechnology **1**, 202 (2005).

[7] Y.A. Kim, T. Hayashi, M. Terrones, M. Endo, M.S. Dresselhaus, Journal of Biomedical Nanotechnology **2**, 106 (2006).

[8] S.C. Ray, A. Saha, N.R. Jana, R. Sarkar, Journal of Physical Chemistry **C 113**, 18546 (2009).

[9] H. Yan, M. Tan, D. Zhang, F. Cheng, H. Wu, M. Fan, X. Ma, J. Wang, Talanta **108**, 59 (2013).

[10] S. Hu, F. Tian, P. Bai, S. Cao, J. Sun, J. Yang, Materials Science and Engineering **B 157**, 11 (2009).

[11] N.G. Semaltianos, S. Logothetidis, N. Frangis, I. Tsiaoussis, W. Perrie, G. Dearden, K.G. Watkins, Chemical Physics Letters **496**, 113 (2010).

[12] N.G. Semaltianos, S. Logothetidis, N. Hastas, W. Perrie, S. Romani, R.J. Potter, G. Dearden, K.G. Watkins, P. French, M. Sharp, Chemical Physics Letters **484**, 283 (2010).

[13] A. Al-Hamaoy, E. Chikarakara, H. Jawad, K. Gupta, D. Kumar, M.S. Ramachandra Rao, S. Krishnamurthy, M. Morshed, E. Fox, D. Brougham, X. He, M. Vazquez, D. Brabazon, Applied Surface Science **302**, 141 (2014).

[14] K. Bagga, R. McCann, M. Wang, A. Stalcup, M. Vazquez, D. Brabazon, Journal of Colloid and Interface Science **447**, 263 (2015).

[15] M. Gill, W. Perrie, A. Papworth, P. Fox, W. O'Neill, Proceedings of SPIE - The International Society for Optical Engineering **5713**, 560 (2005).

[16] X.Y. Xu, R. Ray, Y.L. Gu, H.J. Ploehn, L. Gearheart, K. Raker, W.A. Scrivens, Journal of the American Chemical Society **126**, 12736 (2004).

[17] S.N. Baker, G.A. Baker, Angewandte Chemie International Edition **49**, 6726 (2010).

[18] G.W. Yang, Progress in Materials Science **52**, 648 (2007).

[19] L. Yang, P.W. May, L.Yin, J.A.Smith, K.N. Rosser, Diamond and Related Materials **16**, 725 (2007).

[20] P.W. May, Philosophical transactions of the Royal Society of London A **358**, 473 (2000).

[21] International Standard ISO13321 Methods for Determination of Particle Size Distribution Part 8: Photon Correlation Spectroscopy, International Organisation for Standardisation (ISO) 1996,

[22] International Standard ISO22412 Particle Size Analysis – Dynamic Light Scattering, International Organisation for Standardisation (ISO) 2008,

[23] R. Meilunas, R.P.H. Chang, S. Liu, M. Jensen, M.M. Kappes, Journal of Applied Physics **70**, 5128 (1991).

[24] A.C. Ferrari, J. Robertson, Physics Review **B 61**, 14095 (2000).

[25] Y. Guo, Z. Wang, H. Shao, X. Jiang, Carbon **52**, 583 (2013).

[26] Y. Wang, A. Hu, Journal of Materials Chemistry **C 2**, 6921 (2014).

[27] H. Li, X. He, Z. Kang, H. Huang, Y. Liu, J. Liu, S. Lian, C.H.A. Tsang, X. Yang, S.T. Lee, Angewandte Chemie International Edition **49**, 4430 (2010).

[28] S.-L. Hu, K.-Y. Niu, J. Sun, J. Yang, N.-Q. Zhao, X.-W. Du, Journal of Materials Chemistry **19**, 484 (2009).

[29] Y. Fang, S. Guo, D. Li, C. Zhu, W. Ren, S. Dong, E. Wang, ACS Nano **6**, 400 (2011).

[30] X.-J. Mao, H.-Z. Zheng, Y.-J. Long, J. Du, J.-Y. Hao, L.-L. Wang, D.-B. Zhou, Spectrochimica Acta Part **A 75**, 553 (2010).

[31] A.B. Bourlinos, R. Zboril, J. Petr, A. Bakandritsos, M. Krysmann, E.P. Giannelis, Chemistry of Materials **24**, 6 (2011).

[32] S. Srivastava, N.S. Gajbhiye, ChemPhysChem **12**, 2624 (2011).

[33] Y. Deng, D. Zhao, X. Chen, F. Wang, H. Song, D. Shen, Chemical Communications **49**, 5751 (2013).

Copyright line will be provided by the publisher